Appl. Phys. 17, 413—416 (1978)

Applied Physics

© by Springer-Verlag 1978

Intensity Enhanced Bulk Photovoltaic Effects in $LiNbO_3$: Fe*

*Dae M. Kim***

Max-Planck-Institut für Festkörperforschung, Stuttgart, Fed. Rep. Germany

J. G. Gallagher, Jr., T. A. Rabson, and *F. K. Tittel*

Electrical Engineering Department, Rice University, Houston, TX 77001, USA

Received 6 December 1977/Accepted 3 March 1978

Abstract. The saturated value of the macroscopic electric field arising from the photocurrent-induced crystal capacitance in $LiNbO_3$: Fe is shown to increase significantly with illuminating intensity. In addition, the current-intensity characteristics is shown to depart appreciably from the linear relationship. These measurements, together with other existing data are interpreted by incorporating in the charge transport process a new secondary photorefractive centers.

PACS: 78.20

The light-induced refractive index change (Δn) in $LiNbO_3$, measured for the first time by Chen et al. [1, 2] showed that the saturated value of Δn depended rather sensitively on the intensity. For instance, at 255 W/cm^2 Δn reached $\sim 10^{-3}$, which nearly amounts to 3 times the value at 64 W/cm^2. The transport mechanism causing this "optical damage" was later described by Glass et al. [3] in terms of the bulk photovoltaic effect. They showed in their investigation of current-voltage characteristics in $LiNbO_3$:Fe that the bias voltage necessary to reduce the photocurrent to zero also depended significantly on intensity: 60 KV/cm at 0.32 W/cm^2 vs. 38 KV/cm at 0.08 W/cm^2. The measurement of the equivalent bulk photovoltaic field in $LiNbO_3$:Fe by phase holography again indicated that the saturated value ($\mathscr{E}_{sat}$) increased substantially with increasing intensity [4]. These series of data appear to suggest a general trend. The dark conductivity (σ_D) causes $\mathscr{E}_{sat}$ to depend on intensity to a certain extent [5]. However, at high intensity regime, its effect is negligible[1]. We present here two additional sets of experimental measurements and interprete this general trend from the single viewpoint within the framework of a bulk photovoltaic effect.

Experiment and Results

First, we measured the electric field associated with the photocurrent-induced crystal capacitance. The crystal chosen was an unannealed $LiNbO_3$:Fe with Fe dopant concentration 0.1%/mole. ($\alpha = 28\,cm^{-1}$)[2]. The physical dimensions are 1×1 [cm] along a, c axes and 0.1 cm along b axis. The crystal was placed in one arm of the Mach-Zehnder interferometer (see insert in Fig. 1) and two optical beams from Ar^+ laser source (488 nm), having approximately equal amplitude and polarized along c-axis were intersected at the center of the crystal surface (half angle $\approx 12°$). The overlapped beam cross sectional diameter was about 0.3 cm. Under this *open* circuit condition, Δn grows with exposure. The evolution in time of the spatially uniform component of Δn was monitored by measuring the fringe shift of the probing weak-intensity He–Ne laser at the center of the overlapped region. In Fig. 1 are presented the corresponding space charge fields (via the electro-optic coefficient) that develop as a

* Supported in part by a National Science Foundation and BMDATC grant.

** On leave of absence from Rice University, Houston, Texas, USA.

[1] For example, in the measurement of the bias voltage by Glass et al., the dark current constituted 3% of the total current at 0.32 W/cm^2, and 13% at 0.08 W/cm^2. To explain the ratio of two measured bias voltages, viz. 1.58, the dark current should be 58% of the total current at 0.08 W/cm^2 rather than mere 13%.

[2] Crystal purchased from Crystal Technology, Inc. Mountain View, Calif.

0340-3793/78/0017/0413/$01.00

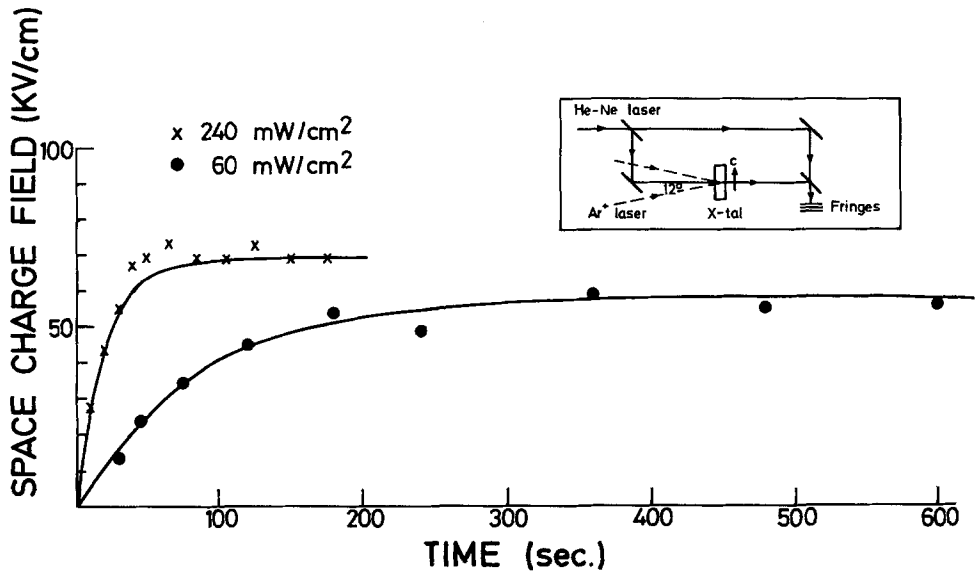

Fig. 1. The space-charge field associated with the photo-current-induced crystal capacitance as a function of writing time for two different intensities. The solid lines are theoretical fit to the data with $\gamma = 1.2\,\mathrm{cm}^2/\mathrm{W}$, $\kappa_1 \alpha I_0/\epsilon\varepsilon_0 = 0.012\,\mathrm{s}^{-1}$ at $I_0 = 60\,\mathrm{mW/cm}^2$, see (8). Insert: Experimental configuration for fringe shift measurement

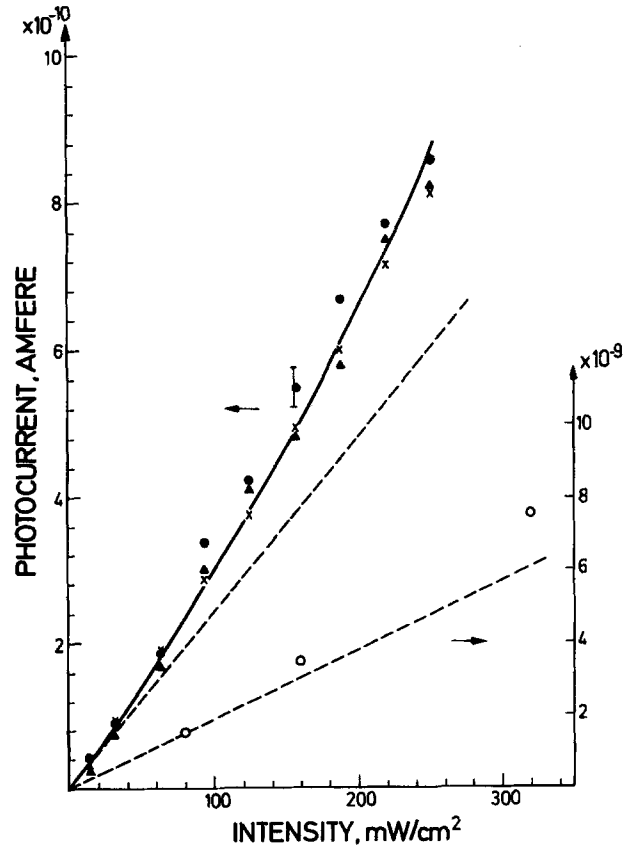

Fig. 2. Photocurrent as a function of intensity. Three different sets of data (●, × ▲) were taken on three different weeks. ○ denotes the data of [7]. The solid line represents the theoretical fit to the data with $\gamma = 1.2\,\mathrm{cm}^2/\mathrm{W}$, the broken line the slope of J w.r.t. I

function of writing time for two different (total) intensities. Note that at $240\,\mathrm{mW/cm}^2$, $\mathscr{E}_{\mathrm{sat}}$ reaches $\approx 70\,\mathrm{KV/cm}$, which is 20% higher than the value at $60\,\mathrm{mW/cm}^2$. This shows that $\mathscr{E}_{\mathrm{sat}}$ depends significantly on intensity whether the writing beam is spatially modulated or uniform [1, 2] or whether the crystal is doped with impurities as in our case or subject to inadvertent impurities [1, 2]. In [1] the dependence of $\mathscr{E}_{\mathrm{sat}}$ on intensity is much more pronounced than our results, perhaps due to the fact that intensities used in [1] were higher than ours by three orders of magnitudes.

Next, the photocurrents with the same crystal under a closed circuit condition were measured. The experimental procedures are well detailed in the literature [3, 6]. The crystal c-surfaces were covered with silver painted electrodes and connected to a low impedance circuit. An expanded 488 nm Ar^+ laser uniformly illuminated the whole crystal surface. Photocurrents were measured for several different intensities with *no* external field applied. σ_D was negligible in our measurement. In Fig. 2 are presented three sets of photocurrents as a function of intensity. Each set of data was taken during the single run, and three different sets were obtained in three different weeks. For a fixed intensity, the photocurrent values vary appreciably among the three different sets, meaning that the reproducibility of the data is poor. However, during each single run the accuracy of the data point is well within 10%. Figure 2 clearly indicates that the measured photocurrents depart significantly from the

linear current-intensity relationship. For comparison, we have also plotted in Fig. 2 photocurrents measured by Glass et al. [7] with no external field applied.

Table 1 summarizes the intensity enhanced values of $\mathscr{E}_{sat}$, the bias voltage, and the photocurrents, as reported by different groups. The general trend mentioned above can be seen clearly from this table.

We next interprete the data. The photo-induced current and the photorefractive effect are attributed to directional charge excitation and transport from Fe^{2+} centers, followed by retrapping at Fe^{3+} sites [3]. In this two-level model, transport theories predict intensity independent $\mathscr{E}_{sat}$ and linear response of photocurrent. $\mathscr{E}_{sat}$ to a certain measure depends on intensity due to a dark current. However, the dark conductivity is negligible at the intensity levels used for most of the measurements in Table 1. We show that the nonlinear effects mentioned above can be accounted for by introducing, in the charge transport process, an intermediate level, that is produced and maintained by the light exposure. The high lying excited levels of Fe^{2+} and Fe^{3+} impurity or the formation of a secondary photorefractive centers may constitute this level. In fact, color centers were reported to be produced during two-photon absorption experiment in $LiNbO_3$ and to affect significantly the ensuing photorefractive process [8]. In addition, a nonlinear light absorption occuring in $LiNbO_3$:Co was attributed to a two-step-process via an intermediate state of Co [9]. Hence, it would appear realistic to introduce a third level in the transport process. This level, in turn, may absorb light and enhance the bulk photovoltaic charge transfer.

The total current then consists of the usual two level photovoltaic term, the dark current (σ_D) and the term contributed by the secondary impurity center, i.e.

$$J=[\kappa_0+\kappa_1(E+\mathscr{E})]\alpha I+\sigma_D(E+\mathscr{E})+J_{int}. \tag{1}$$

Here, κ_0 denotes the bulk photovoltaic coefficient and

$$\kappa_1=(e/h\nu)\mu\tau+\kappa_0\beta \tag{2}$$

incorporates (a) the photoconductivity (μ,τ the mobility and life time of the electron) and (b) the possible modification of κ_0 arising from the lattice polarity change in the presence of external (E) as well as space charge ($\mathscr{E}$) fields [10, 11]; β represents the linear field dependence of κ_0. J_{int} is determined by three factors: i) the excitation rate from the secondary photorefractive center ($\sigma^* I/h\nu$), ii) the net directional charge transport mean free path ($\Lambda^*=l_+^* p_+^* - l_-^* p_-^*$)[3], and iii) the density given in terms of the life time (τ^*) and the quantum

[3] We assume that the secondary impurity center is also in a local asymmetric potential, and the probabilities $p_\pm^*, p_\mp^*$ of intervalence charge transfer in the $\pm c$ directions and the corresponding mean free paths $l_\pm^*, l_\mp^*$ differ.

Table 1. Saturated values of space charge field ($\mathscr{E}_{sat}$), bias field to reduce photocurrent to zero (E_b), and photocurrent at two different intensities and the % difference w.r.t. the lower values

Crystal α, [cm^{-1}]	$\mathscr{E}_{sat}, E_b$ [kV/cm]	Current [PA/mW]	Intensity [mW/cm^2]	Diff. [%]	Ref.
$LiNbO_3$ (<0.22)	23 64		94×10^3 255×10^3	178	[1]
$LiNbO_3$ 0.2 wt-% Fe (38)	38 60		80 320	58	[3]
$LiNbO_3$ 0.05%/mole Fe (12)	11 17		1.5 6	55	[4]
$LiNbO_3$ 0.2 wt-% Fe (45)		20 24	80 320	20	[7]
$LiNbO_3$ 0.1%/mole Fe (28)	58 69		60 240	19	Present result
$LiNbO_3$ 0.1/mole Fe (28)		2.9 3.4	63 220	17	Present result

production efficiency (q) from the primary photoexcitation at Fe^{2+} sites. Thus

$$J_{int}=e\Lambda^*(\sigma^* I/h\nu)[(\alpha I/h\nu)q\tau^*/(1+\sigma^* I(1-q)\tau^*/h\nu)] \cdot[1+(\mu\tau/\Lambda^*)(E+\mathscr{E})] \tag{3}$$

Clearly, J_{int} increases according to I^2 power law. This additional current term, viz. J_{int} can describe the set of data summarized in Table 1. Under a uniform illumination, $I=I_0$ and the closed circuit condition ($\mathscr{E}_{dc}=0$), the current without external field is given by

$$J=\kappa_0\alpha I_0(1+\gamma I_0), \tag{4}$$

where

$$\gamma=e\Lambda^*\sigma^*\tau^*q/[(h\nu)^2\kappa_0(1+\sigma^* I_0\tau^*(1-q)/h\nu)] =(\sigma^*\tau^*/h\nu)\cdot(\Lambda^*/\Lambda)q(1+\sigma^* I_0\tau^*(1-q)/h\nu)^{-1} \tag{5}$$

represents the photovoltaic coefficient at the intermediate level, scaled w.r.t. κ_0; Λ denotes the charge transport mean free path for two level scheme, i.e. $l_+p_+-l_-p_-$ [3]. Equation (4) readily describes the nonlinear current-intensity characteristics measured in our experiment. Under the same conditions, the bias field needed to reduce the photocurrent to zero is

$$E_b=(\kappa_0/\kappa_1)[(1+\gamma I_0)/(1+\sigma_D/\kappa_1\alpha I_0 +\kappa_0\mu\tau\gamma I_0/\kappa_1\Lambda^*)] \tag{6}$$

Note that in the intensity range where σ_D is negligible, E_b still increase with I_0 [3] provided $\kappa_0\mu\tau/\kappa_1\Lambda^*\ll1$. Under an open circuit condition, the crystal capacitance field $\mathscr{E}$ evolves in time as

$$\frac{\partial}{\partial t}\mathscr{E}+J/\epsilon\varepsilon_0=0. \tag{7}$$

With no external field present ($E=0$) and for $I=I_0$ one finds for $\kappa_0\mu\tau/\kappa_1\Lambda^*\ll 1$

$$\mathscr{E}(z,t)=\left(\frac{\kappa_0}{\kappa_1}\right)\frac{1+\gamma I_0}{1+\sigma_D/\kappa_1\alpha I_0}\cdot\{1-\exp[-(\kappa_1\alpha I+\sigma_D)t/\in\varepsilon_0]\}. \quad (8)$$

$\mathscr{E}(z,t)$ grows and saturates in time scale mainly determined by the light intensity. The steady state value of the spatially uniform component of $\mathscr{E}(z,t)$ is given with the neglect of σ_D for simplicity by

$$\mathscr{E}_{\text{sat}}=(\kappa_0/\kappa_1)(1+\gamma I_0). \quad (9)$$

It is clear from (8) and (9) that $\mathscr{E}_{\text{sat}}$ increases with intensity whether the illuminating beam is spatially modulated as in our case or spatially uniform as in the case of Chen et al. [1]. The data reported in [4] can also be interpreted by finding the fundamental component of $\mathscr{E}(z,t)$ in (1). In our analysis we have not considered the effects of external field [12] or the change in the primary impurity densities [13], which have been detailed in the literature.

The coefficient γ appearing in (9) can be determined from the two measured $\mathscr{E}_{\text{sat}}$ values (see Fig. 1). One finds for low intensity regime ($\sigma^*I(1-q)\tau^*/h\nu\ll 1$)

$$\gamma\cong 1.2\,\text{cm}^2/\text{W}. \quad (10)$$

Using the γ-value thus found in (4) one can account for the nonlinear current-intensity characteristics (see Fig. 2)[4]. It should be noted that the coefficient γ depends on many parameters, characteristic of the nature of the secondary photorefractive center, e.g. σ^*, τ^*, and Λ^*. In particular, the effective photovoltaic mean free path Λ^* could be much larger than that of Fe^{2+} centers, i.e. $\kappa_0\mu\tau/\kappa_1\Lambda^*\ll 1$, if the intermediate level lies close to the conduction band edge.

[4] The absolute value of our photocurrent is much smaller than the values reported in the literature for $LiNbO_3$:Fe, perhaps due to contact problems.

Conclusion

In conclusion, we have discussed in this paper the intensity-enhanced bulk photovoltaic effects in $LiNbO_3$ crystals by introducing secondary photorefractive centers. We have shown that, although the origin of these new centers is not clear so far, it is capable of describing various measurements reported in the literature. This effect is of practical importance in that it may improve significantly the photorefractive sensitivity in $LiNbO_3$ crystals. Presently, we are investigating this effect further by writing holograms in pulsed mode of laser operation, and comparing the ensuing photorefractive sensitivity with that of cw hologram recording.

References

1. F.S.Chen, J.T.LaMacchia, D.B.Fraser: Appl. Phys. Lett. **13**, 223 (1968)
2. F.S.Chen: J. Appl. Phys. **40**, 3389 (1969)
3. A.M.Glass, D. von der Linde, T.Negran: Appl. Phys. Lett. **25**, 233 (1974)
4. D.M.Kim, R.R.Shah, T.A.Rabson, F.K.Tittel: Appl. Phys. Lett. **29**, 84 (1976)
5. K.Bløtekjaer: J. Appl. Phys. **48**, 2495 (1977)
6. J.M.Spinhirne, D.Ang, C.S.Joiner, T.L.Estle: Appl. Phys. Lett. **30**, 89 (1976)
7. A.M.Glass, D. von der Linde, D.A.Auston, T.J.Negran: J. Electronic Materials **4**, 915 (1975)
8. D. von der Linde, O.F.Schirmer, H.Kurz: Appl. Phys. **15**, 153 (1978)
9. H.Kurz, D. von der Linde: Ferroelectrics (to be published)
10. H.Kurz: Ferroelectrics **13**, 291 (1976)
11. H.Kurz, E.Krätzig, W.Keune, H.Engelmann, U.Gonser, B.Disehler, A.Räuber: Appl. Phys. **12**, 355 (1977)
12. J.P.Huignard, F.Micheron: Appl. Phys. Lett. **29**, 591 (1976)
13. M.Peltier, F.Micheron: J. Appl. Phys. **48**, 3683 (1977)